Journal of Advanced Chemical Engineering
ISSN: 2090-4568

Abdelaal and Harbrecht, J Adv Chem Eng 2014, 5:1
DOI: 10.4172/2090-4568.1000116

Research Article Open Access

Template-Assisted Synthesis of Metal Oxide Hollow Spheres Utilizing Glucose Derived-Carbonaceous Spheres As Sacrificial Templates

Haitham Mohammad Abdelaal [1*] and Bernd Harbrecht[2]

[1]*Ceramics Department, The National Research Centre, Al-Buhouth St. Dokki, Cairo, Egypt*

[2]*Department of Chemistry and Centre of Materials Science Philipps University, 35032 Marburg, Germany*

Abstract

A series of metal oxides hollow spheres (Cr_2O_3, α-Fe_2O_3, Co_3O_4, NiO and ZnO) have been fabricated using the glucose derived-carbonaceous spheres as sacrificial templates and the metal chlorides as precursors for the metal oxides in a sacrificial templating process. Heating of an aqueous solution of the metal chloride and glucose in an autoclave at 180 ºC affords - as indicated by transmission electron microscopy (TEM) - a nanospherical composite consisting of a metal precursor shell sheathing a carbonaceous core. Consequently, hollow crystalline oxides spheres are obtained by removal of the carbonaceous cores through calcination in air. Correlations between the particle size and the various synthesis conditions such as glucose concentration, the molar concentration ratio between glucose and metal chloride, temperature, reaction time and the addition of acetic acid as a catalyst are uncovered. The obtained metal oxides hollow spheres were characterized by means of scanning electron microscopy (SEM), transmission electron microscopy (TEM), x-ray powder diffraction (XRD), infrared spectroscopy (IR), and nitrogen adsorption/desorption isotherms (BET).

Keywords: Oxides; Chemical techniques; Electron microscopy; Microstructure; Hollow materials

Introduction

Recently, in both academic and technological studies, inorganic oxides hollow spheres are attracting great attention due to their enhanced properties such as hollow cores, large specific surface area and low density a long with the distinct functions of oxides. Therefore, they present a class of distinct materials that provoke new options in the development of diverse potential applications such as protection of sensitive components (as enzymes and proteins), catalysis, coatings, water treatment, encapsulation of chemicals - for controlled-release applications - and adsorption. Moreover, other interesting applications may be proposed based on the chemical and physical characteristics of the inorganic hollow particles [1-12]. A variety of chemical and physicochemical methods such as sol-gel process [13], spray pyrolysis methods [14], surface polymerization processes [15], sonochemical route [16], colloidal templating methods and template free approaches have been used for the fabrication of hollow micro and nanomaterials [17,18]. Among the various synthesis methods, sacrificial templating approaches are considered as the most efficient and often used method for the fabrication of hollow structured micro and nanoparticles. In this way the fabrication of hollow particles usually involves the preparation of core-shell composite particles. These hybrid particles can be formed by precipitation of inorganic precursors of the target oxide hollow particles onto the surface of the core particles followed by etching of the cores by soaking the core in appropriate solvent in case of inorganic templates or thermal treatment in case of organic templates [12].

Various templating agents have been introduced for the fabrication of inorganic hollow materials including silica [19], gold [20], calcium carbonate [21], silver nanoparticles [22], hematite [23], polystyrene (PS) latex [17], polymethylmethacrylate (PMMA) [24], chitosan-polyacrylic acid (CS-PAA) [25], and n-propyle amine [26]. Latterly, carbohydrates such as glucose and sucrose have been used successfully as sacrificial templates for the synthesis of hollow inorganic particles [27-28]. Glucose is considered one of the most promising carbohydrates that can be used as sacrificial templates for the synthesis of inorganic hollow structures as it is one of the most inexpensive and widely available carbohydrates. They have surface functionalities such as -C=O and -OH groups facilitating adsorption of the desired materials onto their reactive surfaces, as have been reported previously for different hollow materials [7,27-29].

In previous work, we have demonstrated the fabrication of silica hollow nanospheres via a facile one pot hydrothermal strategy by applying glucose-derived carbonaceous spheres as sacrificial templates. We further demonstrated that the shell size of hollow spheres can be varied by the variation of the starting materials [30]. Ta_2O_5 hollow nanospheres have been prepared by using glucose as sacrificial templates as well [31]. Further, fructose-derived carbonaceous spheres have been applied as sacrificial templates for the fabrication of some metal oxides hollow submicrospheres via a hydrothermal approach [32].

In this work we report the use of a facile route, hydrothermal hydrolysis, to fabricate porous crystalline metal oxides hollow spheres using glucose derived-carbonaceous spheres as sacrificial templates and metal chlorides as precursors for the metal oxides. In addition, the correlations between the particle size and the various synthesis conditions such as glucose concentration, the molar concentration ratio between the glucose and the metal chloride, temperature, reaction time and the addition of catalyst are investigated.

The interest in the use of monosaccharides, as sacrificial templates to fabricate the hollow metal oxides, arises from the reactive surface

***Corresponding author:** Haitham Mohammad Abdelaal, Ceramics Department, The National Research Centre, Al-Buhouth St. Dokki, Cairo, P.O. Box 12622, Egypt, Tel: 002-010-1674-6660; E-mail: hmaa_77@yahoo.com

Received November 25, 2014; **Accepted** December 23, 2014; **Published** December 31, 2014

Citation: Abdelaal HM, Harbrecht B (2014) Template-Assisted Synthesis of Metal Oxide Hollow Spheres Utilizing Glucose Derived-Carbonaceous Spheres As Sacrificial Templates. J Adv Chem Eng 5: 116. doi: 10.4172/2090-4568.1000116

of the glucose-derived carbonaceous materials - with its richness in O-functionalities - that facilitate the precipitation of the oxide precursor onto their surface layers without any further surface modifications. The former mentioned fact is probably the key to success in fabrication of the hollow spheres. In addition, the synthesis route is simple and can be readily analyzed and manipulated compared with complex multistep strategies including many procedures and a variety of chemical additives.

Experimental

Materials

D-(+)-Glucose monohydrate ($C_6H_{12}O_6 \cdot H_2O$), Chromium (III) chloride hexahydrate ($CrCl_3 \cdot 6H_2O$), cobalt (II) chloride hexahydrate ($CoCl_2 \cdot 6H_2O$), iron (III) chloride hexahydrate ($FeCl_3 \cdot 6H_2O$), zinc(II) chloride ($ZnCl_2$) and nickel(II) chloride ($NiCl_2$) were obtained from Merck (Darmstadt, Germany). All chemicals were analytical grade and employed without further purification. Distilled water (conductivity ~ 1.7 μS cm^{-1}) was used.

Fabrication of the metal oxide hollow spheres

The major process steps applied in the present work involved heating the metal chloride with glucose in closed system results in in-situ formation of hybrid particle due to the adsorption of the metal ions on the surface layers of the glucose-derived carbonaceous spheres. Finally, calcination of the hybrid spheres lead to the formation of hollow metal oxide.

For the formation of the metal oxide hollow spheres, glucose is applied as the sacrificial template, while metal chlorides [chromium (III) chloride hexahydrate ($CrCl_3 \cdot 6H_2O$), iron (III) chloride hexahydrate ($FeCl_3 \cdot 6H_2O$), cobalt(II) chloride hexahydrate ($CoCl_2 \cdot 6H_2O$), nickel(II) chloride ($NiCl_2$), and zinc(II) chloride ($ZnCl_2$)] are the precursors for the desired Cr_2O_3, α-Fe_2O_3, Co_3O_4, NiO and ZnO hollow spheres, respectively.

In a typical synthesis experiment, 1902 mg of glucose was dissolved in 100 mL distilled water. The water soluble metal chloride was added to satisfy the glucose: metal chloride molar ratio 10:1. The mixture was heated in a 100 mL Teflon-lined stainless steel autoclave at 180 °C for 24 *h*. The products were filtered off; washed three times, first with distilled water and then ethanol, and finally dried in a vacuum oven at 60 °C for 5 *h*. After synthesis, the core @ shell composites were calcined in air at 500 °C (heating rate 2 °C min^{-1}, 5 *h*) to remove the carbon core eventually leading to the target metal oxide hollow particles.

Characterization

The resulting hollow metal oxides and their corresponding composites were characterized by infrared (IR) spectra using IFS 88 from Bruker and XRD patterns obtained by using X-ray powder diffraction (X'Pert MPD, Pananalytical) operating in Bragg–Brentano geometry. The diffractometer was equipped with a graphite monochromator at the detector side. The sample holder was a single-crystal silicon plate. The XRD patterns, following Rietveld refinement procedures, were performed with the X'Pert software package supplied by the Pan Analytical Company.

The surface area was studied by nitrogen- sorption measurements performed with use of a Micromeritics ASAP 2020 gas sorptometer. The samples were degassed in vacuum at a pressure of 0.4 Pa for at least 3 *h* at 200 °C prior to measurements at 77 K over a range of relative pressures from 0.01 to 0.995. Specific surface areas were calculated by assuming Brunauer-Emmet-Teller (BET) conditions. The particles morphology was visualized using a JEOL JSM-7500F field emission scanning electron microscope at an accelerating voltage of 5 kV. Therefore, the ground samples were mounted on an aluminium stub covered with a conductive carbon tape. To avoid surface charging the samples were coated with an ultra thin layer of platinum coating before SEM analyses. Transmission electron microscopy (TEM) was conducted with use of an electron microscope (JEM-3010, JEOL) operating at 300 kV. The samples were crushed to a powder and mounted by drop-drying of a chloroform suspension onto TEM cupper grids before TEM analyses.

Results and Discussion

The formation of the porous metal oxides hollow spheres

Figure 1 illustrates schematically the proposed mechanism of the formation of the porous metal oxides hollow spheres. The formation of hollow oxides spheres through the hydrothermal hydrolysis method involves adsorption of the metal ions dispersed in the solution mixture into the hydrophilic surface layers of the glucose-derived carbonaceous spheres which are rich in oxygen functionalities such as -OH and C=O [28-29]. This results in the in-situ formation of a core @ shell composite consisting of glucose-derived carbonaceous spheres with the metal ions bound to the oxygen functionalities in the outer shell; these are finally densified and cross-linked in a subsequent pyrolytic treatment eventually leading to free standing porous hollow metal oxide spheres after the removal of the carbonaceous core materials. The as-obtained hollow metal oxide spheres are replicas of the carbonaceous core spheres though about 60-80% smaller in size than the original corresponding composite granules.

The significant shrinkage in size in the course of the thermal treatment indicates that the composite with the metal cations bound to the carbonaceous spheres (CSs) transformed into a dense network of nanocrystalline metal oxide grains composing the shells of the hollow spheres. Frequently, the hollow spheres products exhibit a ball in ball (bnb) hollow structure which is obtained without any extra step.

The mechanism of the formation of the bnb structure is still vague and a challenge to the material scientists. However, it was postulated that some nano-islands of metal oxide nanoparticles in the shell may migrate to or be stuck on the surface of the shrinking CSs cores in the course of the calcination process at moderate temperature. Additional heating at elevated temperature, these nano-islands finally aggregate into a small ball in the interior when the CSs cores are wholly burnt off [33-34].

Figure 2 shows the XRD patterns of the metal oxide hollow spheres obtained through the typical experimental procedures after calcination at 500 °C for 5 *h*. It shows that, the metal oxide hollow spheres consist of the well crystalline single phase metal oxide as shown by Rietveld refinement of the XRD patterns [35]. The average crystallite size was calculated by applying the Scherrer equation using the full width at half maximum (FWHM) of the most intense peaks [36]. The mean size was determined to be 21, 23, 12, 11, 18 nm for Cr_2O_3, α-Fe_2O_3, Co_3O_4, NiO and ZnO, respectively. No crystalline peaks were observed before calcination (insets in Figure 2) disclosing that the metal ions are evenly adsorbed onto the hydrophilic shell of the carbonaceous cores or disseminated in the shell as amorphous cluster after hydrothermal treatment.

Figure 3 shows TEM micrographs of the products before

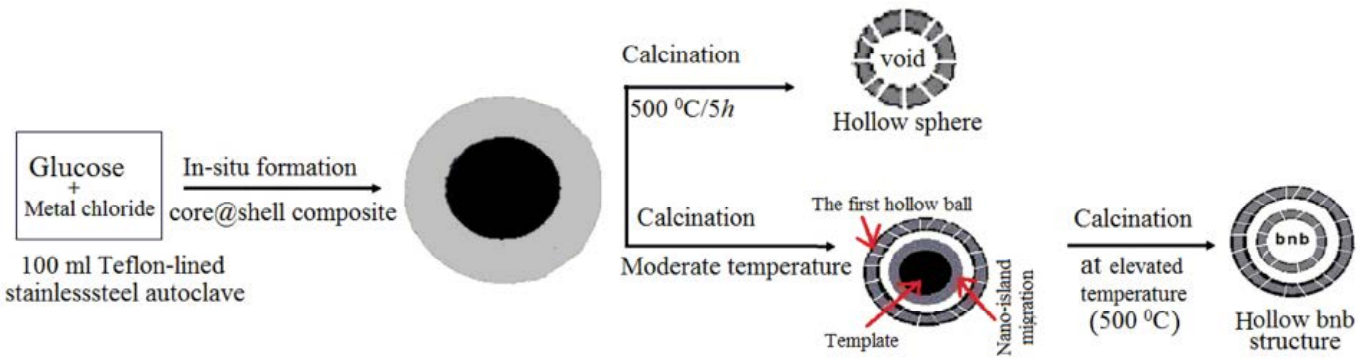

Figure 1: Schematic diagram of the fabrication of porous metal oxide hollow spheres by hydrothermal method.

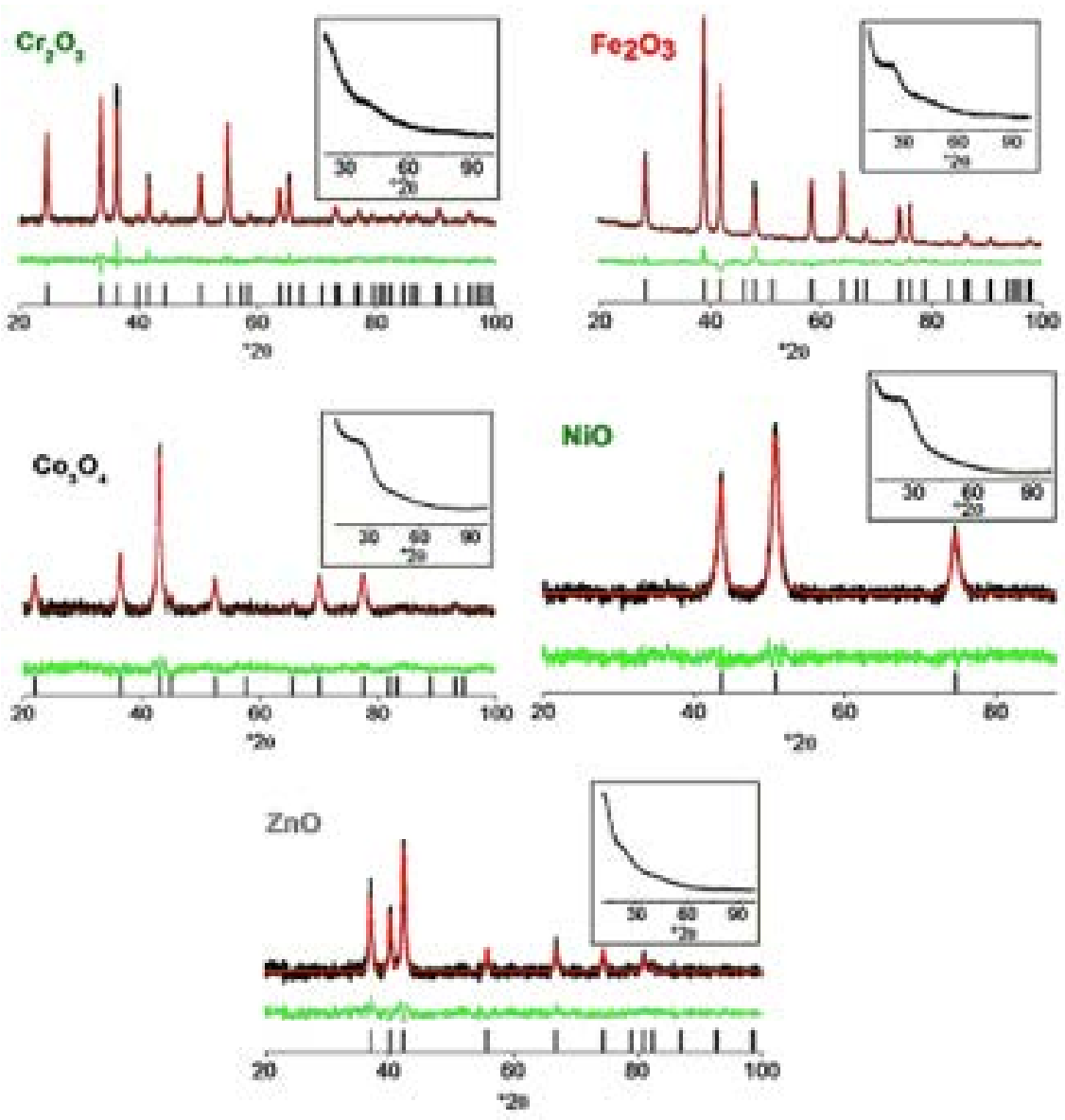

Figure 2: XRD patterns of the as-obtained oxides with Rietveld refinement (the black line is the observed pattern ,the red line is the calculated from the literatures and the green line represents the difference plot, the grey marker indicate possible Bragg positions consistent with the space group symmetry of the metal oxide). The insets show the XRD patterns of the samples before calcination.

calcination. They depict hybrid nature of the core @ shell composite of Cr_2O_3, α-Fe_2O_3 and ZnO samples. We can see that a contrast appears in the micrographs between the shell material and the core material. This provides support for the assumption of the spatial separation of the metal ions rich shell and the carbonaceous cores.

Comparison between IR spectra before and after calcination at 500 °C for 5 *h*, evidence the removal of the carbonaceous cores and the formation of the metal oxide hollow spheres as shown in Figure 4 for α-Fe_2O_3 hollow spheres. The IR spectrum before calcination displays a broad peak at 3400 cm^{-1}, which is attributed to be the stretching vibration of O-H groups. The peak at ~ 2900 cm^{-1} arises from the stretching vibrations of C-H bonds. The modes at 1701 cm^{-1} and 1630 cm^{-1} can be assigned to C=O and C=C, respectively. The C=C double bonds indicate that dehydration has taken place during the hydrothermal carbonization of glucose [37-38].

After calcination the carbonaceous templates and most peaks related to the functionalities, like carboxylic or aromatic groups disappeared and the observed peaks are typically related to M-O stretching vibrations as shown in Figure 4 which represents the IR spectrum of α-Fe_2O_3 hollow spheres. The observed bands at 570 and 480 cm^{-1} are typical for Fe-O modes of hematite α-Fe_2O_3 [39].

SEM micrographs in Figure 5 a, b and d, e display the metal oxide hollow particles before and after calcination of Cr_2O_3 and α-Fe_2O_3 respectively. SEM micrographs of the products Figure 5 b, e and Figure S2 (Supporting Information) evidence the formation of the spherical hollow metal oxides particles. The surface of the hollow spheres shows that the hollow metal oxides spheres walls are composed of many small nanoparticles of the metal oxide. From the broken shell, marked with a red arrow, we can notice the hollow porous nature of the metal oxides hollow spheres.

From Figure 5 a, b, d, e and also Figure S2 we can notice that after calcination the spheres preserve the three dimensional spherical shape of particles after removing of the carbonaceous core. In addition, about 60-80% shrinkage in size occurs after calcination as can be seen from the particle size distribution of the metal oxide hollow spheres and their corresponding composites (Figure S3). Apparently, the metal ions incorporated in the surface layer of the template densify and cross-link in the course of the pyrolysis to form the metal oxide hollow spheres replicas of the carbonaceous spheres template with significantly reduced size.

TEM micrographs (Figure 5 c, f, g, h, i) of Cr_2O_3, α-Fe_2O_3, Co_3O_4, NiO and ZnO, respectively, further confirm clearly the hollow interior as indicated by variation of the contrast between the dark shell and the pale core. The wall thickness of the porous hollow metal spheres can be estimated according to the cross sectional view obtained by TEM micrographs to be approximately 80 nm, 40 nm, 20 nm, 30 nm, and 18 nm for Cr_2O_3, α-Fe_2O_3, Co_3O_4, NiO and ZnO hollow spheres, respectively.

In general, SEM and TEM micrographs disclosed the formation of uniform hollow metal oxide spheres. Moreover, they reveal the formation of a ball in ball (bnb) hollow structure (Figures 5 and S4), as well. The high resolution TEM micrographs of Cr_2O_3, Co_3O_4, and ZnO porous hollow spheres (Figure S5) show that the size of the small nanoparticles composing the wall of the hollow spheres are in good agreement with the size calculated by the Scherrer equation for the as-obtained metal oxide hollow spheres.

The nitrogen adsorption/desorption isotherms were applied to study specific surface area of the hollow metal oxides spheres (Figure S6). The observed hysteresis loops in the curves of all samples demonstrate the presence of mesoporous structures. They are typical isotherms characteristic of mesoporous materials according to the International Union of Pure and Applied Chemistry (IUPAC) [40]. The surface areas of the hollow oxides were 77, 54, 35, 33 and 65 m^2g^{-1} for Cr_2O_3, α-Fe_2O_3, Co_3O_4, NiO and ZnO hollow spheres, respectively. The specific surface area of the hollow metal oxides results from the sum of the areas of the outer and interior surface of the hollow spheres and the surface of the primary pores. The large surface areas and the spherical hollow shape that can be manipulated with respect to size, wall thickness and porosity makes this kind of materials interesting for various potential applications in several fields.

The impact of the synthesis conditions

Temperature (T), reaction time (*t*), concentration of glucose, the concentration ratio between glucose and metal chloride, and addition of acetic acid as catalyst are found to be five significant parameters that affect the outcome of the hydrothermal process. To study the impact of each synthesis parameter the experimental conditions were systematically varied whereby the parameter under investigation was varied while the other parameters remained unchanged according to the optimized synthesis procedures.

The results show that each parameter of the previously mentioned parameters has, to a large degree, a similar impact on the formation of the different types of oxides. The similar influence of each parameter on the formation of the hollow oxide spheres reported here might open the door for an improved understanding of the formation of the hollow metal oxide spheres with variable size.

The optimal temperature (T) for the formation of the hollow oxides using glucose as sacrificial templates is 180 °C. When decreasing T to 170 °C or raising it to 200 °C, no significant precipitates were seen at the former and no hollow spheres were formed at the latter temperature in all oxides under investigation. The optimal time (*t*) for the formation of metal oxide hollow spheres was 24 *h*. In case of increasing time to 36 *h* no hollow materials were observed except for Cr_2O_3 which formed fused hollow particles. While decreasing *t* to 12 *h*, the only observed hollow spheres were those for Cr_2O_3 with average size ~210 nm (Figures 6 a1, a2 and Figures S7 a).

Increasing glucose concentration from 96 $mmolL^{-1}$ - the typical glucose concentration- to 240 $mmolL^{-1}$ resulted in the formation of fused hollow particles for the oxides under investigation (Figures 6 b1 and b2; Figures S7 b, c and d). On the other hand, decreasing the glucose concentration to 64 $mmolL^{-1}$ resulted in small hollow spheres dispersed in nanoparticles of the metal oxide (Figure S7 e).

Figure 7 illustrates the impact of adding 0.5 mL of acetic acid to the reaction mixture solution. It is obvious that acetic acid catalyzes the reaction and increases the rate of the hydrothermal reaction and as a result the average size of the metal hollow oxides spheres increases by about 40-50%.

When the concentration ratio between glucose and metal chloride is increased from 10:1 to 20:1, we can anticipate that the amount of metal oxide forming the shell of hollow spheres will decrease. Figure 8 shows TEM micrographs for as-obtained hollow Cr_2O_3 samples through applying concentration ratio of 10:1 and 20:1. We notice that the wall thickness of the hollow spheres is inversely proportional to the molar ratio between the reactants. The wall thickness decreases from 80 nm to 33 nm when the concentration ratio increases. The particle size of the Cr_2O_3 particles forming the wall of the hollow spheres is found

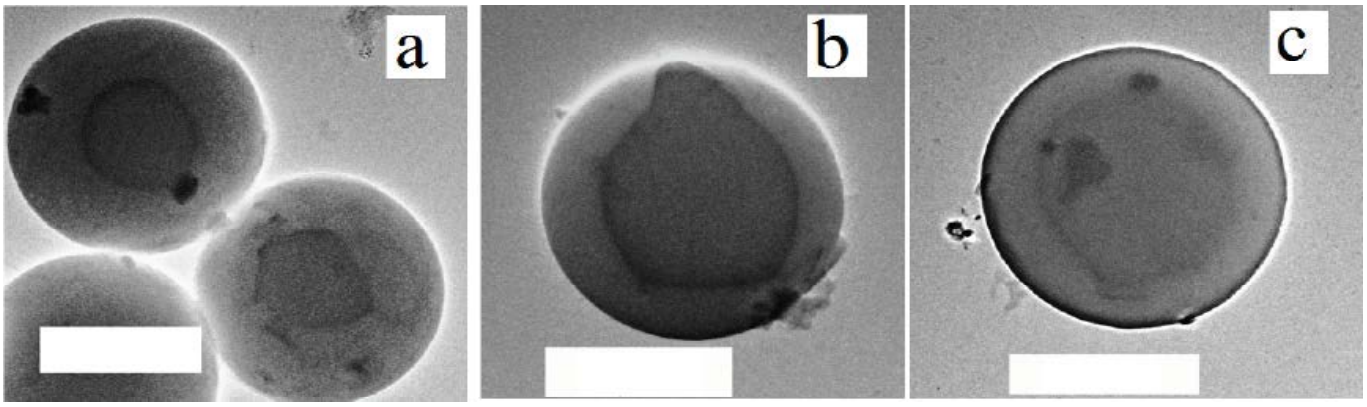

Figure 3: TEM micrographs of the core @ shell composites before calcination of a) Cr_2O_3, b) α-Fe_2O_3, c) ZnO samples; the scale bare is 1 μm.

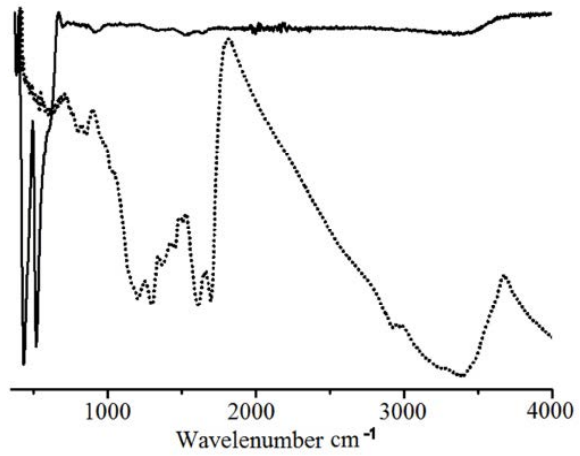

Figure 4: IR spectra of the as-obtained α-Fe_2O_3 hollow spheres, before and after calcination (500 ˚C, 5 h)..... before calcination; —— after calcination.

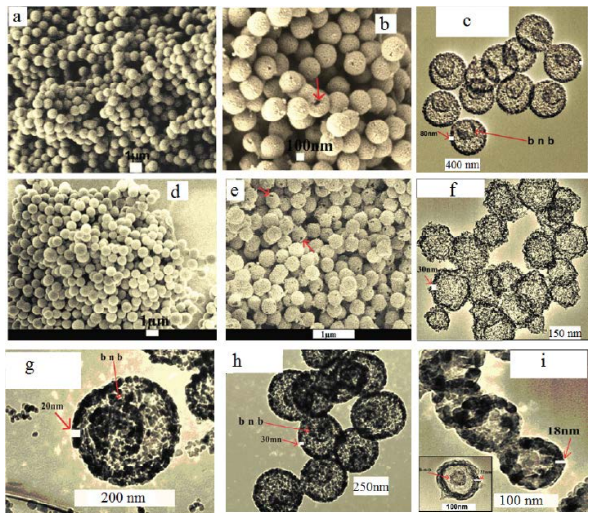

Figure 5: SEM micrographs of the core-shell composites before calcination at 500 ºC (a) Cr_2O_3 and (d) α-Fe_2O_3, SEM micrographs of the oxide hollow spheres after calcination at 500 ºC for 5 *h* (b) Cr_2O_3 and (e) α-Fe_2O_3, and TEM micrographs of the oxide hollow spheres (c) Cr_2O_3 (f) α-Fe_2O_3 (g) Co_3O_4 (h) NiO (i) ZnO the inset TEM micrograph shows bnb hollow structure of ZnO.

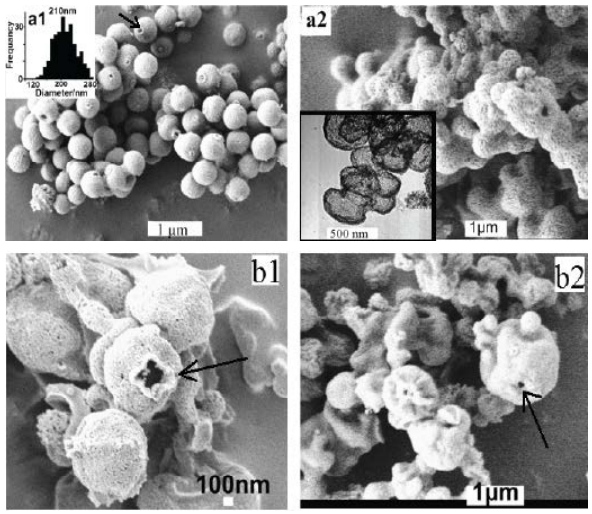

Figure 6: SEM micrographs of the metal oxide hollow particles, after calcination at 500 ˚C for *5 h*, a1) hollow Cr_2O_3 spheres prepared at 12 *h* (the inset is PSD of the sample), a2) fused hollow Cr_2O_3 particles prepared at 36 *h* (the inset is TEM micrograph of the sample), and SEM micrographs of fused hollow porous metal oxide prepared by using 240 $mmoL^{-1}$ of glucose after calcination at 500 ˚C for *5 h*, b1) Cr_2O_3, b2) Co_3O_4. The arrows point to a broken shell.

to be approximately 21 nm. Hence, the 80 nm large walls of the hollow spheres are built up by about four layers of aggregated Cr_2O_3 grains for samples with higher Cr content (ratio 10:1). In contrast, lower Cr content (ratio 20:1) yields hollow spheres with walls consisting of nearly 2 layers of aggregated grains. Accordingly, the hollow spheres appear to be more robust in case of lower molar ratios (glucose/metal chloride). This is likely due to lower metal concentration leads to light packing of metal oxide nanoparticles and a thin wall, while an increase in the metal ions concentration yields a much denser packing and the formation of a robust thicker shell [29].

In general, the size of the hollow spheres is directly proportional to the reaction time and the addition of acetic acid (0.5 mL/100 mL solution) promoting the growth of the spherical core @ shell composite. While the wall thickness of the hollow spheres is inversely proportional with the increase of the molar ratio between glucose and metal chloride. The shape of the hollow materials is affected by the glucose concentration. The typical parameters given by the synthesis protocol procedures reported in experimental section are the optimized conditions for the fabrication of porous hollow metal oxides by using

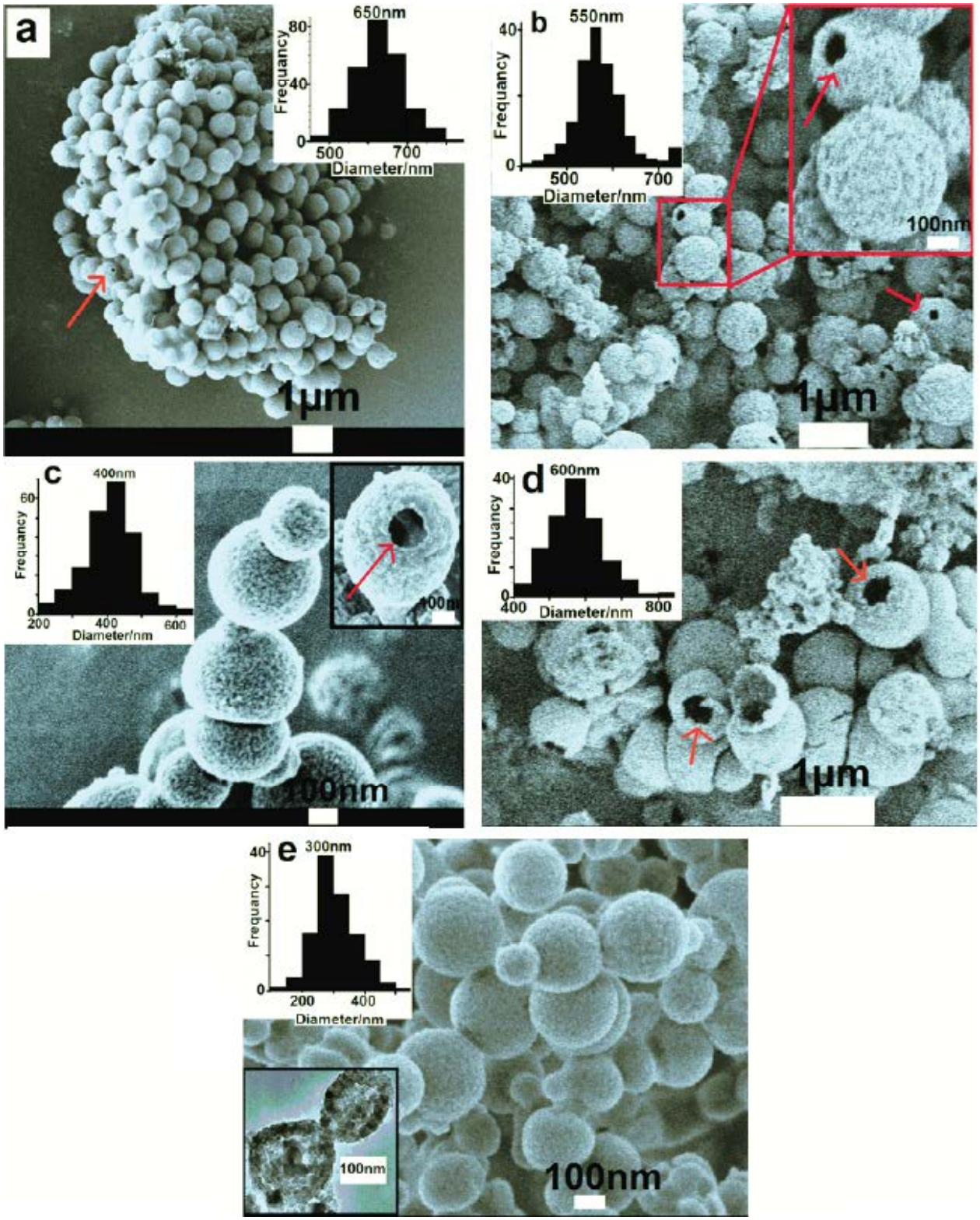

Figure 7: SEM micrographs of porous metal oxide hollow spheres prepared by applying 0.5 mL acetic acid as catalyst, after calcination at 500 ˚C for 5 *h*, a) Cr_2O_3, b) α-Fe_2O_3, the inset is a large view of the chosen area, c) Co_3O_4, the inset is SEM micrograph of a single hollow spheres with broken shell, d) NiO, and e) ZnO, the inset is TEM micrograph of hollow ZnO spheres; the particle size distribution of each sample is included in each micrograph. The red arrow refers to broken shells.

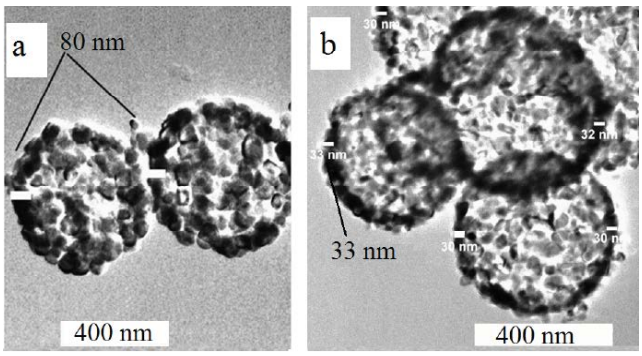

Figure 8: TEM micrographs of the as-obtained Cr_2O_3 hollow spheres by applying concentration ratio [c (glucose):c(metal chloride)] a) 10: 1 b) 20:1.

glucose as a sacrificial template. Table S2 in the Supporting Information summarizes some relationships between the synthesis parameters and the size and shape of the as-obtained hollow metal oxides spheres.

Conclusion

A series of porous metal oxides hollow spheres (Cr_2O_3, Co_3O_4, NiO, α-Fe_2O_3 and ZnO) have been successfully obtained through hydrothermal method by utilizing glucose-derived carbonaceous spheres as sacrificial templates and metal chlorides as metal oxides precursors. The key of success probably stems from the fact that the surface of the carbonaceous core is rich of functionalities which facilitate the adsorption of the metal ions into their surface layers without any surface modifications. The glucose-derived carbonaceous spheres used as templates have an integral and uniform surface functional layer which makes an additional modification of the surface of the shape-controlling carbonaceous template dispensable and provides the homogeneity of the shell. Though the pyrolytic treatment of the composites results in a drastic shrinkage in size, the spherical shape is preserved.

Correlations between the particle size and the concentration of glucose, as well as the ratio of metal precursor and the sugar concentrations are uncovered. Crucial factors, critical to fine-tune the final particle size and the shape, are temperature, reaction time and addition of acetic acid promoting particle growth. The results have shown that each of the varied parameters have similar impact on the various oxides. The similar impact of each parameter on the formation of hollow oxides reported here might open the door for improved understanding of the formation of the hollow metal oxides spheres with variable size.

Metal oxide particles of this type exhibit unique properties such as large specific surface areas and, in particular, hollow interior cores, and mesoporous walls of various size and thickness. In view of the rich and diverse property profiles of such nanoparticulate oxides the accruing properties arising from the specific shape and constitution of such hollow particles may offer improved and new useful applications in various fields. Catalysis, water treatment, photonic devices, chemical sensors and controlled release are just some of those.

References

1. Ludtke S, Adam T, Unger KK (1997) Application of 0.5µm porous silanized silica beads in electrochromatography. J Chromatogr A 786: 229-235.
2. Caruso F (2000) Hollow capsule processing through colloidal templating and self-assembly. Chemistry 6: 413-419.
3. Abdelaal HM (2014) Facile hydrothermal fabrication of nano-oxide hollow spheres using monosaccharides as sacrificial templates. ChemistryOpen.
4. Yuan J, Laubernds K, Zhang Q, Suib SL (2003) Self-assembly of microporous manganese oxide octahedral molecular sieve hexagonal flakes into mesoporous hollow nanospheres. J Am Chem Soc 125: 4966-4967.
5. Zhu Y, Shi J, Shen W, Dong X, Feng J, et al. (2005) Stimuli-responsive controlled drug release from a hollow mesoporous silica sphere/polyelectrolyte multilayer core-shell structure. Angew Chem Int Ed Engl 44: 5083-5087.
6. Zhu Y, Chen H, Wang Y, Li Z, Cao Y, et al. (2006) Mesoscopic photonic crystals made of TiO2 hollow spheres connected by cylindrical tubes. Chem Lett 35: 756-757.
7. Sun X, Liu J, Li Y (2006) Use of carbonaceous polysaccharide microspheres as templates for fabricating metal oxide hollow spheres. Chemistry 12: 2039-2047.
8. Yu J, Liu S, Yu H (2007) Microstructures and photoactivity of mesoporous anatase hollow microspheres fabricated by fluoride-mediated self-transformation. J Catal 249: 59-66.
9. Yu J, Yu H, Guo H, Li M, Mann S (2008) Spontaneous formation of a tungsten trioxide sphere-in-shell superstructure by chemically induced self-transformation. Small 4: 87-91.
10. Chen C, Abbas SF, Morey A, Sithambaram S, Xu L, et al. (2008) Controlled synthesis of self-assembled metal oxide hollow spheres via tuning redox potentials: versatile nanostructured cobalt oxides. Adv Mater 20: 1205-1209.
11. Yuan J, Zhang X, Qian H (2010) A novel approach to fabrication of superparamagnetite hollow silica/magnetic composite spheres. J Magn Magn Mater 322: 2172-2176.
12. Yuan J, Zhou T, Pu H (2010) Nano-sized silica hollow spheres: preparation, mechanism analysis and its water retention property. J Phys Chem Sol 71: 1013-1019.
13. Tissot I, Reymond J, Lefebvre F, Bourgeat-Lami E (2002) SiOH-functionalized polystyrene latexes. A step toward the synthesis of hollow silica nanoparticles. Chem Mater 14: 1325-1331.
14. Messing GL, Zhang SC, Jayanthi GV (1993) Ceramic powder synthesis by spray-pyrolysis. J Am Ceram Soc 76: 2707-2726.
15. Emmerich O, Hugenberg N, Schmidt M, Sheiko SS, Baumann F, et al. (1999) Molecular boxes based on hollow organosilicon micronetworks. Adv Mater 11: 1299-1303.
16. Dhas NA, Suslick KS (2005) Sonochemical preparation of hollow nanospheres and hollow nanocrystals. J Am Chem Soc 127: 2368-2369.
17. Shiho H, Kawahashi N (2000) Iron Compounds as Coatings on Polystyrene Latex and as Hollow Spheres. J Colloid Interface Sci 226: 91-97.
18. Mao LJ, Liu CY, Li J (2008) Template-free synthesis of VOx hierarchical hollow spheres. J Mater Chem 18: 1640-1643.
19. Salgueirino-Maceira V, Spasova M, Farle M (2005) Water-stable, magnetic silica–cobalt/cobalt oxide–silica multishell submicrometer spheres. Adv Funct Mater 15: 1036-1046.
20. Zhang R, Hummelgard M, Olin H (2010) Carbon nanocages grown by gold templating. Carbon 48: 424-430.
21. Zhang S, Li X (2004) Synthesis and characterization of CaCO 3@SiO2 core-shell nanoparticles. Powder Tech 141: 75-79.
22. Sun Y, Xia Y (2002) Shape-controlled synthesis of gold and silver nanoparticles. Science 298: 2176-2179.
23. Han YS, Jeong GY, Lee SY, kim HK (2007) Hematite template route to hollow-type silica spheres. J Sol State Chem 180: 2978-2985.
24. Kato T, Ushijima H, Katsumata M, Hyodo T, Shimizu Y, et al. (2002) Fabrication of hollow alumina microspheres via core/shell structure of polymethylmethacrylate/alumina prepared by mechanofusion. J Mat Sci 37: 2317-2321.
25. Tasi M, Li MJ (2006) A novel process to prepare a hollow silica sphere via chitosan-polyacrylic acid (CS-PAA) template. J Non Cryst Sol 352: 2829-2833.
26. Song L, Ge X, Wang M, Zhang Z (2006) Direct preparation of silica hollow spheres in a water in oil emulsion system: The effect of pH and viscosity. J Non Cryst Sol 352: 2230-2235.
27. Sun X, Li Y (2004) Colloidal carbon spheres and their core/shell structures with noble-metal nanoparticles. Angew Chem Int Ed Engl 43: 597-601.

28. Abdelaal HM (2014) Fabrication of hollow silica microspheres utilizing a hydrothermal approach. Chin Chem Lett. 25: 627-629.

29. Titirici MM, Antonietti M, Thomas A (2006) A Generalized synthesis of metal oxide hollow spheres using a hydrothermal approach. Chem Mater 18: 3808-3812.

30. Abdelaal HM, Zawrah MF, Harbrecht B (2014) Facile one-pot fabrication of hollow porous silica nanoparticles. Chemistry 20: 673-677.

31. Abdelaal HM, Pfeifer E, Grünberg C, Harbrecht B (2014) Synthesis of tantalum pentoxide hollow spheres utilizing a sacrificial templating approach. Matt Lett 136: 4-6.

32. Abdelaal HM, Harbrecht B (2014) Fabrication of metal oxide hollow spheres using fructose derived-carbonaceous spheres as sacrificial templates. C R Chim.

33. Suh WH, Jang A, Suh Y, Suslick KS (2006) Porous, hollow, and ball-in-ball metal oxide microspheres: preparation, endocytosis, and cytotoxicity. Adv Mater 18: 1832-1837.

34. Qian H, Lin G, Zhang Y, Gunawan P, Xu R (2007) A new approach to synthesize uniform metal oxide hollow nanospheres via controlled precipitation. Nanotech 18: 355602.

35. X'Pert Plus (1999) Program for Crystallography and Rietveld analysis, Philips Analytical, Almelo (The Netherlands).

36. Klug HP, Alexander LE (1974) X-ray Diffraction procedures. Wiley: New York, USA.

37. Ni D, Wang L, Sun Y, Guan Z, Yang S, et al. (2010) Amphiphilic hollow carbonaceous microspheres with permeable shells. Angew Chem Int Ed Engl 49: 4223-4227.

38. Sakaki T, Shibata M, Miki T, Hirosue H, Hayashi N (1996) Reaction model of cellulose decomposition in near-critical water and fermentation of products. Bioresour Technol 58: 197-202.

39. Pradhan GK, Parida KM (2011) Fabrication, growth mechanism, and characterization of Î ± -Fe(2)O(3) nanorods. ACS Appl Mater Interfaces 3: 317-323.

40. Sing KSW, Everett DH, Haul RAW, Moscou L, Pierotti RA, et al. (1985) Reporting physisorption data for gas/solid systems with special reference to the determination of surface area and porosity (Recommendations 1984). Pure Appl. Chem. 57: 603-619.